Composite Structures 203 (2018) 164–171

Contents lists available at ScienceDirect

Composite Structures

journal homepage: www.elsevier.com/locate/compstruct

Damage identification for plate-like structures using ultrasonic guided wave based on improved MUSIC method

Hao Zuo, Zhibo Yang, Caibin Xu, Shaohua Tian, Xuefeng Chen*

School of Mechanical Engineering, Xi'an Jiaotong University, Xi'an, PR China
The State Key Laboratory for Manufacturing Systems Engineering, Xi'an, PR China

ARTICLE INFO

Keywords:
Damage identification
Guided wave
Improved MUSIC method
Composite structures

ABSTRACT

The ultrasonic guided wave has emerged as one of the most prominent and promising tools for metal and composite structures in the fields of structural health monitoring (SHM) and nondestructive testing (NDT). This paper presents a novel model-based 2D multiple signal classification (MUSIC) damage identification algorithm for plate-like structures. Unlike the conventional MUSIC algorithm, the proposed model-based 2D MUSIC damage identification algorithm is deduced based on the assumption of near-field according to the propagation model of guided waves. Since scattered signals contain the location information of damage, the cross-correlation function of residual signals received by experiment and scattered signals received by damage scattering model are developed for spatial spectrum estimation MUSIC algorithm. Due to the uncorrelation of signal and noise, the damage can be successfully identified by searching the peak point of spatial spectrum in the monitored area employing the orthogonality of signal subspace and noise subspace. The accuracy and effectiveness of the proposed method are firstly validated by numerical simulation on aluminum plate, and the general applicability is further verified by experiments for the damage identification of laminated composite plate. The numerical and experimental results demonstrate the proposed damage identification algorithm is appropriate for damage identification of plate-like structures with high estimation accuracy and resolution.

1. Introduction

In-situ monitoring of composite structures for damage is urgently needed to improve safety, reliability and operational life in application of aircrafts, warships and pipelines over the most recent two decades [1–3]. Ultrasonic guided wave can propagate in large area for a significant distance with little attenuation and they are also high sensitive to both surface and subsurface discontinuities caused by damage [4,5]. Moreover, the cheap and easy-to-use piezoelectric transducers, which can both generate and receive guided wave, make it possible to inspect large plate-like structures for damage quickly, efficiently and cost-effectively with reasonably transducer layout. These outstanding advantages make guided wave be acknowledged as one of the most prominent and promising tools for large plate-like structures inspection in the fields of structural health monitoring (SHM) and nondestructive testing (NDT).

The primary objective of guided wave based SHM technique is to detect and localise damages in concerned area. However, since the multi-mode and dispersion characteristics of guided waves make the received raw wave packets overlap echoes from damage and boundary degrading the temporal resolution of guided waves and interpreting the received signals hard [6–8] in reality, the challenge of damage detection and localization still remains. Among the published literatures, the guided waves based SHM technique always employs residual signals acquired after baseline substation to interrogate the status of the monitored structure [9]. The tomography imaging technique was firstly proposed for images of aluminum containing holes by Jansen [10]. Both time-of-flight and amplitude of difference signals are extracted for tomographic image reconstruction. Although the tomography imaging technique locates defect with high spatial resolution and image resolution due to fine mechanical scanning indexing, the sensitivity and resolution of tomography imaging technique are dependent on the density of transducers significantly [11]. Besides, the scanning hardware is bulky and expensive which are also the main limitations of tomography imaging technique [12]. Another widespread technique named delay-and-sum (DAS) method introduced by Wang provides a simple and efficient imaging method for locating structural damages [13]. In this technique, each pixel value meshed in monitored area is computed by summing amplitude of time-of-flight from differenced signals and the maximum pixel value indicates the most likely location

* Corresponding author at: School of Mechanical Engineering, Xi'an Jiaotong University, Xi'an, PR China.
E-mail address: chenxf@xjtu.edu.cn (X. Chen).

https://doi.org/10.1016/j.compstruct.2018.06.100
Received 28 January 2018; Received in revised form 21 May 2018; Accepted 25 June 2018
Available online 05 July 2018
0263-8223/

of damage. Inspired by basic idea of DAS, Michaels introduced adaptively computing signal weighting coefficients in pixel intensity calculation and incorporated Minimum Variance Distortionless Response (MVDR) into the algorithm to reduce imaging artifacts and improve imaging resolution [14–16]. The correlation analysis based algorithm named reconstruction algorithm for probabilistic inspection of defects (RAPID) was developed for defect detection, size estimation and localization in complex aircraft wing structures [17]. The RAPID method uses the signal difference coefficient (SDC) value to describe the probability of the damage presence between various transmitter-receiver pairs in ultrasonic sparse array which is the main difference from other guided waves based SHM techniques [18].

With the array signal processing techniques becoming more sophisticated, the multiple signal classification (MUSIC) has been widely applied in radar, sonar, biomedicine, seismic exploration and other fields in recent years [19–22]. The conventional MUSIC algorithm was firstly proposed to estimate the far-field signal parameters by Schmit [23] in 1982. The basic idea of MUSIC algorithm, which is based on the uncorrelation of signal and noise, is to decompose the covariance matrix of array signals to signal subspace and noise subspace by performing eigenvalue decomposition. And then the orthogonality of signal subspace and noise subspace are employed to estimate the direction of arrival (DOA) signal. The MUSIC algorithm has been demonstrated to locate point targets with high-resolution images of scatterers separated by fractions of a wavelength [24]. Labyed developed time-reversal with MUSIC (TR-MUSIC) using the time windowing method to improve image quality [25]. Qian proposed a pseudo-noise resampling (PR) based unitary root-MUSIC algorithm for DOA estimation which combined the unitary root-MUSIC and PR techniques to form a DOA estimator bank and a corresponding root estimator bank [26]. Liang presented a high-order MUSIC algorithm to estimate parameters of mixed sources which required high computation complexity for constructing two fourth-order cumulant matrixes [27]. To overcome the shortages of mixed source localization algorithm, Wang developed mixed-order MUSIC method to provide the improved accuracy of parameter estimation [28]. The proposed method had moderate computation complexity and higher resolution than traditional methods. Recently, the MUSIC method is extended to the field of SHM and applied for impact localization on aluminum plate [29]. Zhong and his coworkers have carried out a lot of remarkable investigations for impact localization on composite structures using uniform linear sensor array [30–32]. The uniform linear sensor array based MUSIC technology is a promising method because of its directional scanning ability and easy arrangement of the sensor array [33]. However, the monitoring range of uniform linear sensor array based MUSIC method is not covered the whole azimuth range 0–360°, and its beamforming properties degrade at angles close to 0° and 180° [34]. These shortcomings can be overcame by adopting cross sensor array and uniform circular sensor array. These planar array not only provide more control and optimization parameters for improving the array beamforming and array performance, but also are more versatile and able to perform full range 360° scanning [35]. For these reasons, a novel two-dimensional plum-blossom sensor array based MUSIC method was proposed for omnidirectional impact localization of composite structures by Zhong [36].

However, the conventional MUSIC algorithm can only get high resolution and estimation accuracy based on incoherent narrowband signals and in far-field assumption. In far-field assumption, the source is so far away from transducers that the wave fronts from source are planar waves. The damage in structures can be regarded as secondary wave source near the transducers and the wave fronts of guided waves are spherical waves which is the main difference with far-field assumption. So the conventional MUSIC algorithm is not suitable for damage inspection of structures. For the sake of damage localization, the model-based 2D MUSIC damage identification algorithm for plate-like structures is proposed combining the wave propagation model with MUSIC method based on near-filed assumption.

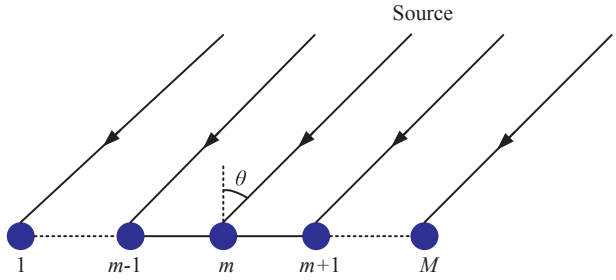

Fig. 1. The model of uniform linear array in far-field condition.

The following sections are organized as follows. The conventional MUSIC algorithm is introduced briefly in Section 2. The proposed model-based 2D MUSIC damage identification algorithm for plate-like structures based on near-filed assumption is presented in Section 3. The numerical simulation and experimental verification are presented in Section 4. The conclusions are given in Section 5.

2. MUSIC algorithm model

Based on far-field assumption, the observed signal arriving at the transducer array can be regarded as planar waves as shown in Fig. 1. Assume a uniform linear array composes of M isotropic transducers and the array element spacing is d. The wave source direction is θ. Taken the mth transducer as referential array element, the delay time τ_i^{far} between the ith array element and referential array element can be written as

$$\tau_i^{far} = \frac{(i-m)d\sin\theta}{c} \quad i = 1, 2, \ldots, M \tag{1}$$

where c denotes wave velocity.

According to the principle of wave propagation, the wave signal $\boldsymbol{s}_i^{far}(t)$ received by the ith array element can be obtained based on referential array element

$$\boldsymbol{s}_i^{far}(t) = \boldsymbol{s}(t)e^{-j2\pi f_0 \tau_i^{far}} \tag{2}$$

where f_0 is frequency of wave source. The exponent part in Eq. (2) can be defined as far-field array steering vector

$$a_i^{far}(\theta) = e^{-j2\pi f_0 \tau_i^{far}} \tag{3}$$

Therefore, the response $\boldsymbol{x}_i^{far}(t)$ received from uniform linear array can be expressed as

$$\boldsymbol{x}_i^{far}(t) = \boldsymbol{s}_i^{far}(t) + \boldsymbol{n}_i(t) \tag{4}$$

where $\boldsymbol{n}_i(t)$ represents noise.

By substituting Eqs. (1)–(3) into Eq. (4), the response $\boldsymbol{x}_i^{far}(t)$ can be rewritten as matrix form

$$\boldsymbol{X}^{far}(t) = \boldsymbol{A}^{far}(\theta)\boldsymbol{s}(t) + \boldsymbol{N}(t) \tag{5}$$

with

$$\boldsymbol{X}^{far}(t) = [\boldsymbol{x}_1^{far}(t), \boldsymbol{x}_2^{far}(t), \cdots, \boldsymbol{x}_M^{far}(t)]^T$$

$$\boldsymbol{A}^{far}(\theta) = [a_1^{far}(\theta), a_2^{far}(\theta), \cdots, a_M^{far}(\theta)]^T$$

$$\boldsymbol{N}(t) = [\boldsymbol{n}_1(t), \boldsymbol{n}_2(t), \cdots, \boldsymbol{n}_M(t)]^T$$

The signal and noise are uncorrelated and independent, so the covariance matrix of response $\boldsymbol{X}^{far}(t)$ received from uniform linear array is

$$\boldsymbol{C}^{far} = E[\boldsymbol{X}^{far}(t)\boldsymbol{X}^{far\,H}(t)] = \boldsymbol{A}^{far}\boldsymbol{C}_S\boldsymbol{A}^{far\,H} + \sigma^2\boldsymbol{I}_N \tag{6}$$

where $\boldsymbol{C}_S = E[\boldsymbol{s}(t)\boldsymbol{s}^H(t)]$ is the covariance matrix of signal with dimension $M \times M$, H denotes complex conjugate transpose and σ^2 is noise power.

According to MUSIC algorithm, the covariance matrix $\boldsymbol{C}^{\text{far}}$ can be decomposed into two orthogonal subspaces named signal subspace and noise subspace by performing eigenvalue decomposition

$$\boldsymbol{C}^{\text{far}} = \boldsymbol{U}\sum\boldsymbol{U}^{\text{H}} = \boldsymbol{U}_S\sum\nolimits_S\boldsymbol{U}_S^{\text{H}} + \boldsymbol{U}_N\sum\nolimits_N\boldsymbol{U}_N^{\text{H}} \tag{7}$$

where $\boldsymbol{U}$ are eigenvectors with $\boldsymbol{U} = [\boldsymbol{e}_1, \boldsymbol{e}_2,\ldots, \boldsymbol{e}_M]$ and $\boldsymbol{\Sigma}$ are eigenvalues with $\boldsymbol{\Sigma} = \text{diag}[\lambda_1, \lambda_2, \ldots,\lambda_M]$. The eigenvalues can be arranged in descending order

$$\lambda_1 \geqslant \lambda_2 \geqslant \cdots \geqslant \lambda_k \geqslant \lambda_{k+1} = \lambda_{k+2} = \cdots = \lambda_M \tag{8}$$

where k is the number of wave sources.

So $\boldsymbol{U}_S$ denotes signal subspace spanned by eigenvectors corresponding to the first k largest eigenvalues $\boldsymbol{\Sigma}_S = \text{diag}[\lambda_1, \lambda_2, \ldots,\lambda_k]$ with expression

$$\boldsymbol{U}_s = [\boldsymbol{e}_1, \boldsymbol{e}_2, \cdots,\boldsymbol{e}_k] \tag{9}$$

And $\boldsymbol{U}_N$ denotes noise subspace spanned by the other eigenvectors corresponding to the smallest eigenvalue $\boldsymbol{\Sigma}_S = \text{diag}[\lambda_{k+1}, \lambda_{k+2}, \ldots,\lambda_M]$ with expression

$$\boldsymbol{U}_N = [\boldsymbol{e}_{k+1}, \boldsymbol{e}_{k+2}, \cdots,\boldsymbol{e}_M] \tag{10}$$

Then multiply covariance matrix $\boldsymbol{C}^{\text{far}}$ by noise subspace $\boldsymbol{U}_N$ for Eqs. (6) and (7), the following expression can be obtained

$$\boldsymbol{A}^{\text{far}}\boldsymbol{C}_S\boldsymbol{A}^{\text{far H}}\boldsymbol{U}_N = 0 \tag{11}$$

As $\boldsymbol{C}_S$ is a full rank matrix, Eq. (11) is written as

$$\boldsymbol{A}^{\text{far H}}\boldsymbol{U}_N = 0 \tag{12}$$

In other words, the far-field array steering vector $\boldsymbol{A}^{\text{far}}(\theta)$ and noise subspace $\boldsymbol{U}_N$ are orthogonal with expression as

$$\boldsymbol{A}^{\text{far H}}\boldsymbol{U}_N\boldsymbol{U}_N^{\text{H}}\boldsymbol{A}^{\text{far}} = 0 \tag{13}$$

The far-filed array spatial spectrum is employed to depict orthogonal property mentioned above

$$P_{\text{MUSIC}}^{\text{far}}(\theta) = \frac{1}{\boldsymbol{A}^{\text{far H}}\boldsymbol{U}_N\boldsymbol{U}_N^{\text{H}}\boldsymbol{A}^{\text{far}}} \tag{14}$$

The direction of arrival (DOA) of wave source can be determined successfully by varying θ to gain the peak point on the spatial spectrum MUSIC in Eq. (14). Because only one parameter needed to be determined in Eq. (14), the far-filed array spatial spectrum is also regarded as 1D MUSIC algorithm.

3. Model-based 2D MUSIC algorithm

It is desired to detect damage in plate-like structures with array signal processing. The scattered signals contain the location information of damage, so the scattered signals are always used to detect damage.

The damage in structure can be considered as secondary wave source which is not always far away from transducer array. Thus the observed signal arriving at transducer array should be regarded as spherical wave to locate the position of damage accurately with near-field assumption.

The uniform linear transducer array for plate-like structure in near-field condition is shown in Fig. 2. Suppose that guided wave is excited at foreknown location $\text{P}_0(\theta_0, R_0)$ with central frequency f_0, and the excitation waveform is known as $\boldsymbol{s}_0$(t). For intact plate-like structure, the received responses from transducer array are only the directly arrival guided waves shown in Fig. 2(a). The damage in structures is always regarded as scattering source, so the received responses from transducer array are composed of the directly arrival guided waves and scattered signals from damage shown in Fig. 2(b) for plate-like structure with damage.

Considering the intact plate-like structure without damage, the measured waveform $\boldsymbol{s}_i^{\text{direct}}(t)$ received from uniform linear transducer array can be expressed as [37]

$$\boldsymbol{s}_i^{\text{direct}}(t) = \frac{1}{2\pi}\int_{-\infty}^{+\infty}\boldsymbol{S}_0(\omega)e^{\frac{-j2\pi f r_i}{c(f)}}\text{d}\omega \tag{15}$$

where $\boldsymbol{S}_0(\omega)$ is the Fourier transform of the excitation $\boldsymbol{s}_0$(t), $c(f)$ denotes the guided velocity which varies by frequency f, r_i is the distance of the wave source P_0 to each array element which can be expressed as

$$r_i = \sqrt{[R_0\sin\theta_0 - (i-m)d]^2 + (R_0\cos\theta_0)^2} \tag{16}$$

However, there is a damage located at unknown location $\text{P}(\theta, R)$ which can be regarded as a second scattering source. The scattered signals can be acquired by means of guided wave propagation model. Due to the existence of damage, the measured waveform $\boldsymbol{s}_i(t)$ received from uniform linear array is composed of two components named the direct signal $\boldsymbol{s}_i^{\text{direct}}(t)$ and the scattered signal $\boldsymbol{s}_i^{\text{scattered}}(t)$ from damage

$$\boldsymbol{s}_i(t) = \boldsymbol{s}_i^{\text{direct}}(t) + \boldsymbol{s}_i^{\text{scattered}}(t) = \boldsymbol{s}_i^{\text{direct}}(t) + \frac{1}{2\pi}\int_{-\infty}^{+\infty}\boldsymbol{S}_0(\omega)e^{\frac{-j2\pi f(r_0+R_i)}{c(f)}}\text{d}\omega \tag{17}$$

with

$$r_0 = \sqrt{(R_0\cos\theta_0 - R\cos\theta)^2 + (R_0\sin\theta_0 - R\sin\theta)^2} \tag{18}$$

$$R_i = \sqrt{R^2 + (i-m)^2d^2 - 2R(i-m)d\sin\theta} \quad i = 1, 2, \cdots, M \tag{19}$$

where r_0 is the distance of wave source P_0 to damage P and R_i is the distance of damage P to each array element.

Thus the scattered signals acquired by means of guided wave propagation model can be written as

$$\boldsymbol{s}_i^{\text{scattered}}(t) = \boldsymbol{s}_i(t) - \boldsymbol{s}_i^{\text{direct}}(t) = \frac{1}{2\pi}\int_{-\infty}^{+\infty}\boldsymbol{S}_0(\omega)e^{\frac{-j2\pi f(r_0+R_i)}{c(f)}}\text{d}\omega \tag{20}$$

The scattered signals in Eq. (20) can also be rewritten as

$$\boldsymbol{s}_i^{\text{scattered}}(t) = \frac{1}{2\pi}\int_{-\infty}^{+\infty}\boldsymbol{S}_0(\omega)e^{\frac{-j2\pi f(r_0+R+R_i-R)}{c(f)}}\text{d}\omega = \boldsymbol{s}_m^{\text{scattered}}(t)e^{\frac{-j2\pi f(R_i-R)}{c(f)}} \tag{21}$$

where the exponent part in Eq. (21) can be defined as near-field array steering vector

$$a_i^{\text{near}}(\theta, R) = e^{\frac{-j2\pi f(R_i-R)}{c(f)}} \tag{22}$$

Ignoring environmental factors, the scattered signal caused by damage can also be obtained by subtracting the baseline signals $\boldsymbol{s}_i^{\text{baseline}}(t)$ (typically damage-free) from measured signals $\boldsymbol{s}_i^{\text{measured}}(t)$ by experiment. Generally, the baseline signals would be prerecorded and the residual signals $\boldsymbol{s}_i^{\text{residual}}(t)$ can be regarded as the scattered signals $\boldsymbol{s}_i^{\text{scattered}}(t)$ with noise

$$\boldsymbol{s}_i^{\text{residual}}(t) = \boldsymbol{s}_i^{\text{measured}}(t) - \boldsymbol{s}_i^{\text{baseline}}(t) = \boldsymbol{s}_i^{\text{scattered}}(t) + \boldsymbol{n}_i(t) \tag{23}$$

Since the scattering pattern contains phase shift errors about scatter, this phase mismatch leads to poor imaging performance [38]. So the analytical representation of scattered signals are employed to reduce the phase mismatch by using Hilbert transform. Thus the cross-correlation function for scattered signals $\boldsymbol{s}_i^{\text{scattered}}(t)$ and residual signals $\boldsymbol{s}_i^{\text{residual}}(t)$ is calculated due to the uncorrelation of signal and noise according to spatial spectrum estimation MUSIC algorithm.

$$\boldsymbol{C}^{\text{near}} = E[\boldsymbol{X}^{\text{scattered}}(t)\boldsymbol{X}^{\text{residual H}}(t)] \tag{24}$$

with

$$\boldsymbol{X}^{\text{scattered}}(t) = [h\{\boldsymbol{s}_1^{\text{scattered}}(t)\},\ h\{\boldsymbol{s}_2^{\text{scattered}}(t)\}, \cdots, h\{\boldsymbol{s}_M^{\text{scattered}}(t)\}]^{\text{T}}$$

$$\boldsymbol{X}^{\text{residual}}(t) = [h\{\boldsymbol{s}_1^{\text{residual}}(t)\},\ h\{\boldsymbol{s}_2^{\text{residual}}(t)\}, \cdots, h\{\boldsymbol{s}_M^{\text{residual}}(t)\}]^{\text{T}}$$

where $h\{\cdot\}$ denotes Hilbert transform.

The covariance matrix $\boldsymbol{C}^{\text{near}}$ can also be decomposed into two orthogonal subspaces named signal subspace and noise subspace by

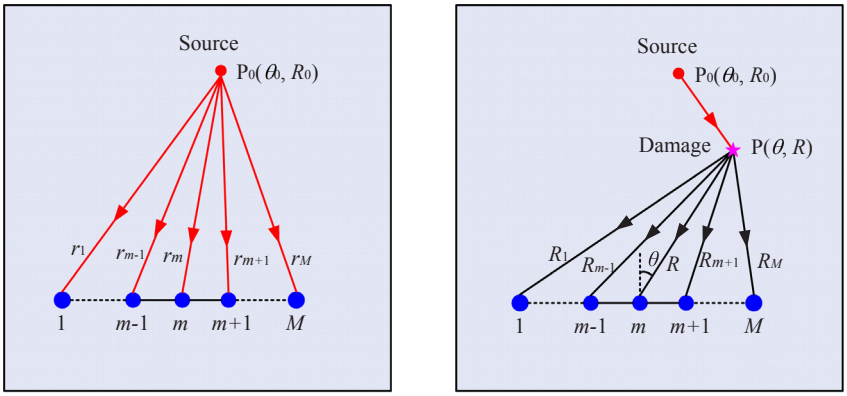

(a) intact plate-like structure (b) plate-like structure with damage

Fig. 2. The uniform linear transducer array for plate-like structure in near-field condition.

performing eigenvalue decomposition

$$\boldsymbol{C}^{\text{near}} = \boldsymbol{U}\sum\boldsymbol{U}^{\text{H}} = \boldsymbol{U}_S\sum\nolimits_S\boldsymbol{U}_S^{\text{H}} + \boldsymbol{U}_N\sum\nolimits_N\boldsymbol{U}_N^{\text{H}} \tag{25}$$

where $\boldsymbol{U}_S$ denotes signal subspace obtained by eigenvector corresponding to the first largest eigenvalue $\boldsymbol{\Sigma}_S$ and $\boldsymbol{U}_N$ denotes noise subspace obtained by eigenvector corresponding to the other eigenvalues $\boldsymbol{\Sigma}_N$.

Similar to the far-field condition, the orthogonality of signal subspace $\boldsymbol{U}_S$ and the noise subspace $\boldsymbol{U}_N$ leads to the following formula for near-field condition

$$\boldsymbol{A}(\theta,\ R)^{\text{H}}\boldsymbol{U}_N = 0 \tag{26}$$

with

$$\boldsymbol{A}(\theta,\ R) = [a_1^{\text{near}}(\theta,\ R),\ a_2^{\text{near}}(\theta,\ R),\ \cdots,\ a_M^{\text{near}}(\theta,\ R)]^{\text{T}}$$

The near-field spatial spectrum is employed to describe orthogonality of near-field array steering vector $\boldsymbol{A}(\theta, R)$ and noise subspace $\boldsymbol{U}_N$

$$P_{\text{MUSIC}}^{\text{near}}\left(\theta,\ R\right) = \frac{1}{\boldsymbol{A}(\theta,\ R)^{\text{H}}\boldsymbol{U}_N\boldsymbol{U}_N^{\text{H}}\boldsymbol{A}(\theta,\ R)} \tag{27}$$

The position parameters of damage can be determined successfully by varying θ and R to scan the whole inspected area. Unlike far-field assumption, two different parameters, θ and R, are required to be determined the position parameters of the damage in near-filed array spatial spectrum in Eq. (27). So the near-filed array spatial spectrum in Eq. (27) is named as model-based 2D MUSIC near-filed array spatial spectrum. The peak point obtained by model-based 2D MUSIC near-filed array spatial spectrum indicates the estimation position parameters of damage.

The general overview of guided wave model-based 2D MUSIC spatial spectrum algorithm under the near-field condition is give in Fig. 3. The detailed steps are as follows:

Step 1: The experiments are implemented on intact and cracked plate-like structures to acquiring baseline signals and measured signals, and then the differential signals are obtained by subtracting baseline signals from measured signals.
Step 2: The inspected area is meshed with $n \times n$ grids.
Step 3: The scattered signals are calculated by Eq. (21) according to the guided wave propagation model.
Step 4: The correlation coefficient of differential signal and scattered signal for referential array element is calculated. The spot of damage is sparse in the whole structure, the most area of structure is intact. So the lower correlation coefficient is considered as non-damage position by setting a threshold to avoiding false prediction, the eigenvalue and the spatial spectrum operations are not needed to be executed which will improved imaging efficiency.
Step 5: If the correlation coefficient is larger than 0.95, the noise subspace $\boldsymbol{U}_N$ is obtained by performing eigenvalue decomposition of covariance matrix $\boldsymbol{C}^{\text{near}}$ and the spatial spectrum $P_{\text{MUSIC}}^{\text{near}}(\theta,\ R)$ is calculated by Eq. (27). Or the spatial spectrum $P_{\text{MUSIC}}^{\text{near}}(\theta,\ R)$ is considered as non-damage position.
Step 6: Scan the next node and repeat Step 3-Step 5.
Step 7: Draw the spatial spectrum and find the peak to locate damage.

4. Algorithm verification

The proposed model-based 2D MUSIC algorithm for damage identification is firstly validated by numerical simulation. Then experiments on laminated composite plate structure are also conducted for damage detection.

4.1. Numerical validation

In order to demonstrate the validity and accuracy of proposed model-based 2D MUSIC algorithm, the numerical simulation is firstly implemented on an aluminum plate with material parameter density $\rho = 2690\ \text{kg/m}^3$, Young's modulus $E = 68.9$ GPa and Poisson's ratio $\upsilon = 0.33$. The high frequency guided waves are more sensitive with small damage, so a 5-cycle Hanning windowed tone burst centered at 50 kHz is selected as excitation signal with time domain and frequency domain waveform shown in Fig. 4(a). The dimension parameters of aluminum plate are illustrated in Fig. 4(b). The excitation is applied at the central of plate and the uniform linear transducer array, which is consisted of seven measuring points with spacing 10 mm, is 200 mm away from transmitter.

The simulation is performed on CUDA platform via GPU-based wavelet finite element method which can be found in [39]. Firstly, the baseline signals were recorded under the intact aluminum plate without damage. Then the damage was added in simulation and the measured signals were also recorded. Thus the scattered signals caused by damage can be obtained by measured signal after baseline subtraction.

In order to evaluate the performance of proposed damage location algorithm, the damage location error can be defined as the distance of actual damage to identified damage

$$r_{\text{error}} = \sqrt{(x^*-x)^2 + (y^*-y)^2} \tag{28}$$

where (x^*, y^*) and (x, y) denote the positions of actual damage and identified damage, respectively.

The spatial spectrum of damage identified results for aluminum plate using model-based 2D MUSIC algorithm are shown in Fig. 5(a) without threshold and Fig. 5(b) with threshold 0.95 for actual damage

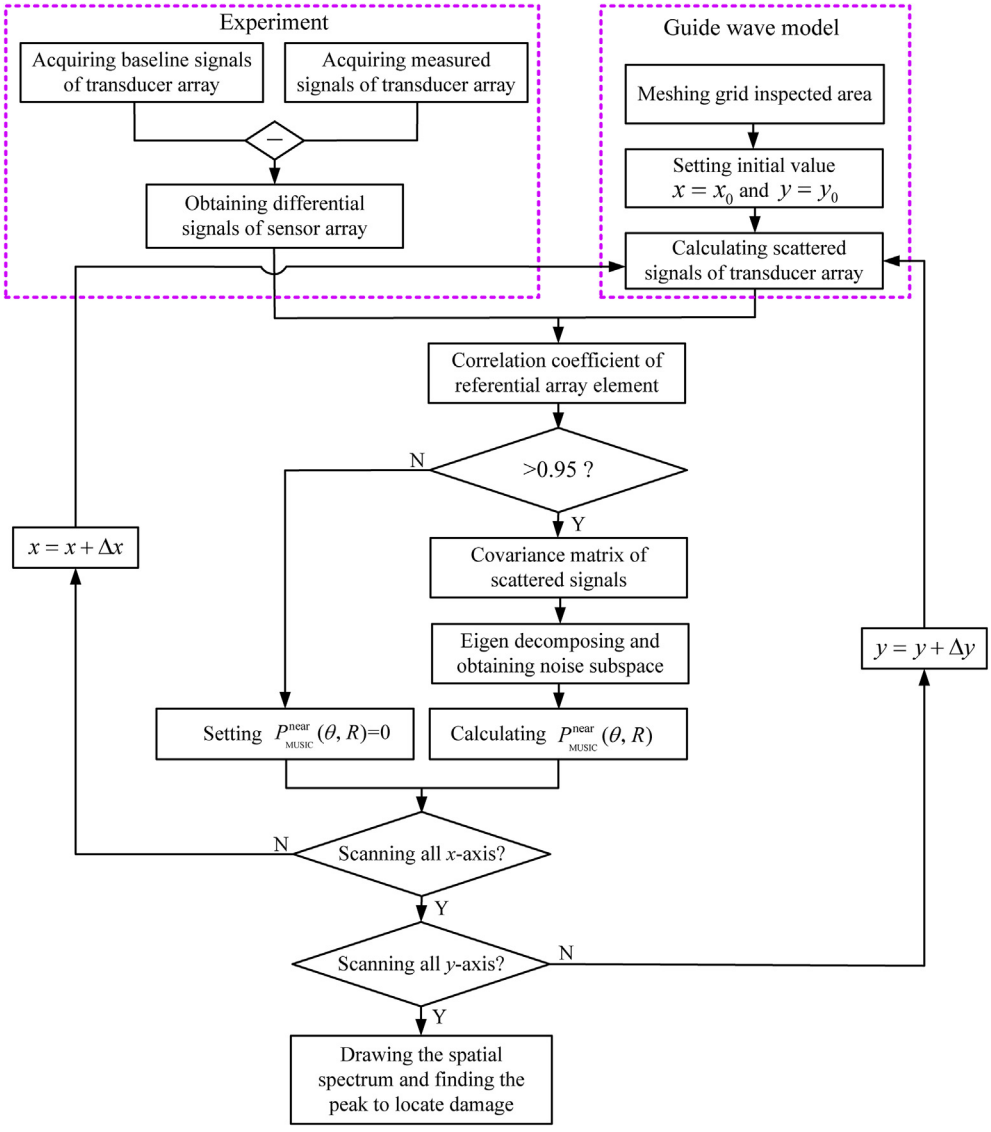

Fig. 3. The guided wave model-based 2D MUSIC spatial spectrum algorithm under the near-field condition.

D in Fig. 4(b) with position (−100 mm, 100 mm). The Cartesian coordinate system is used for better comparison with DAS. It should be noted that the red dot denotes the position of high frequency narrow band impulse and the green dots represent the position of recorded signals. The recorded signals are composed of seven groups with spacing 10 mm. As seen in Fig. 5(a), the actual damage has been identified with position (−100 mm, 95.0 mm) successfully which is 5.0 mm location error away from actual damage. Different from Fig. 5(a), the threshold can decrease the spot size of damage identification and the estimated damage position is also (−100 mm, 95.0 mm)

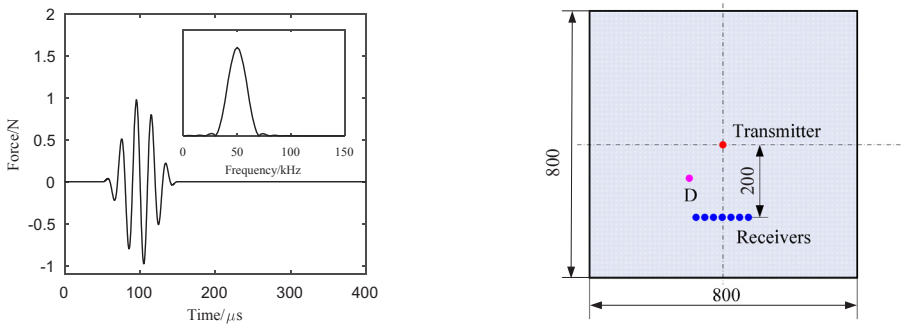

(a) The high frequency excitation signal (b)The dimension parameters of aluminum plate

Fig. 4. The high frequency excitation signal and dimension parameters of aluminum plate.

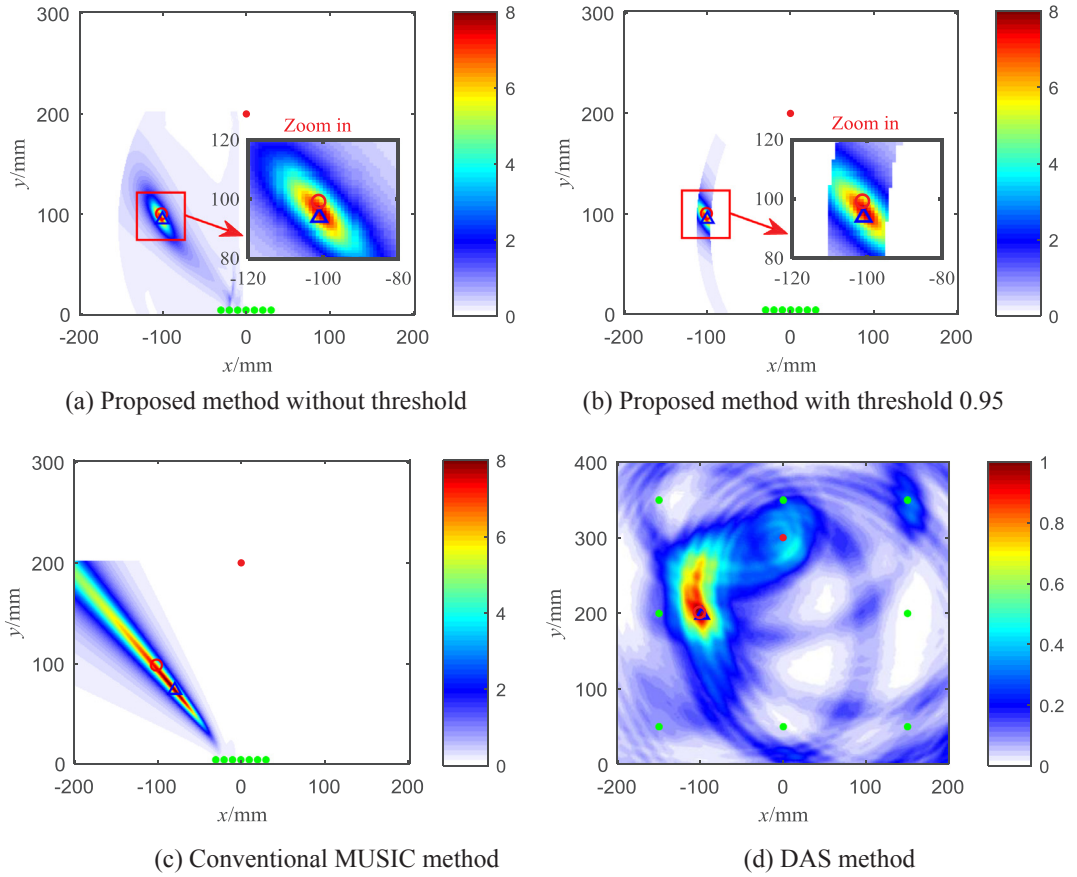

Fig. 5. The results of damage identification (the red circle denotes actual damage position and the blue triangle denotes identified damage position). (For interpretation of the references to colour in this figure legend, the reader is referred to the web version of this article.)

in Fig. 5(b). The location error is so small that the identified damage position is almost coincide with actual simulated damage position. The identified damage has high resolution and the damage location can be distinguished clearly. However, the conventional MUSIC [31] identifying damage with position (−79 mm, 74 mm) is also presented in Fig. 5(c). The location error is 33.4 mm which is larger than that identified by the proposed model-based 2D MUSIC algorithm in this paper. Furthermore, the result obtained by widely used DAS is also presented in Fig. 5(d). Although, the DAS method can recognize the damage with high accuracy, the resolution is not better than the proposed model-based 2D MUSIC algorithm.

In brief, the proposed model-based 2D MUSIC algorithm achieves highly precise positioning result as well as high resolution which is appropriate for damage identification of plate-like structures.

4.2. Experimental validation

In this section, the proposed model-based 2D MUSIC algorithm is then applied to composite plate for damage detection. The experiment is performed on a 16-layered anisotropic $[0^\circ/45^\circ/-45^\circ/90^\circ]_{2s}$ CF/EP laminated composite plate with material parameters $E_1 = 94.1$ GPa, $E_2 = E_3 = 7.76$ GPa, $G_{12} = G_{13} = 2.53$ GPa, $G_{23} = 2.7$ GPa, $\nu_{23} = 0.43$, $\nu_{12} = \nu_{13} = 0.31$, $\rho = 1442\,\mathrm{kg/m^3}$. The detail experimental specimen and setup are illustrated in Fig. 6. The dimensional parameters are 400 mm × 400 mm × 2 mm. There are eight 0.5 mm thickness and 8 mm diameter piezoceramics affixed on the surface of the laminated composite plate with one served as transmitter and the others served as receivers. The transducer array is composed of seven transducers with spacing 10 mm as shown in Fig. 6(a) and the specimen is placed on four small foams for free boundary conditions. The fourth transducer is regarded as referential array element where is also the origin of coordinates. The experimental setup is mainly composed of NI PXI platform including NI PXI-5412 waveform generator and NI PXI-5122 digitizer, PIEZO EPA-104 linear amplifier as shown in Fig. 6(b).

The 5-cycle Hanning window tone burst with central frequency 30 kHz signal is performed as excitation signal to obtain single A_0 mode signal and the sampling frequency is 10 MHz. To simulate damage, two 10 mm diameter cylindrical magnets are affixed on the laminated composite plate. For this reason, it is very convenient to simulate various damage position parameters by changing the positions of magnets.

Firstly, the baseline data was recorded under the intact laminated composite plate without damage and the wave velocity was calculated as 1220 m/s according to the time-of-flight of signals [16]. Then the magnets were affixed on laminated composite plate to record the measured signals. Thus the scattered signals caused by damage can be obtained by measured signal after baseline subtraction.

Two different damages with position D1(28 mm, 170 mm) and D2(−100 mm, 100 mm) shown in Fig. 6(a) were simulated using magnets. The spatial spectrum of damage identified results for laminated composite plate using model-based 2D MUSIC algorithm are shown in Fig. 7 where the actual damages are also presented. As seen in Fig. 7, the two simulated damages have been recognized successfully with identified damage position (27 mm, 169 mm) for D1 and (−97 mm, 103 mm) for D2. The identified damages have been recognized with highly precise positioning results, so the identified results are very close to actual damages, especially for D1.

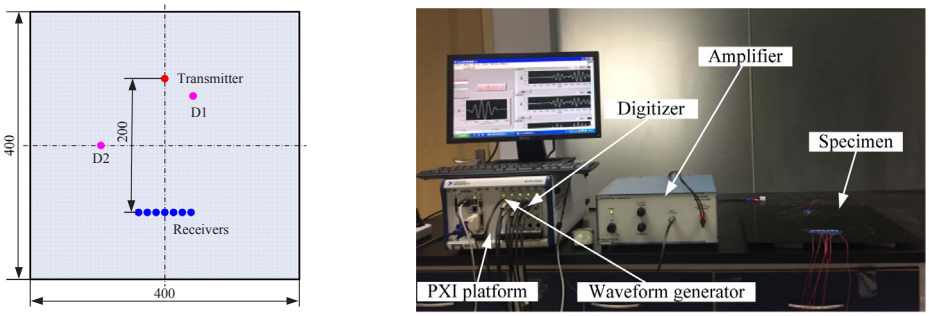

(a)transducer arrangements of laminated composite plate (b) experiment setup

Fig. 6. Experimental transducer arrangements and setup of laminated composite plate.

In order to verify the widely applicability of the proposed model-based 2D MUSIC damage identification algorithm, more experiments were performed on the same laminated composite plate with simulated damages listed in Table 1. All the damages have been successfully identified with identified position results listed in Table 1. Furthermore, the identified results are also illustrated in Fig. 8 where the corresponding actual damages are also presented. The identified results in case 1–6 achieve ideal results with the maximum location error 5.0 mm. Although cases 7 and 8 show larger location error comparing with other cases, the identified results are also still acceptable with maximum location error 8.1 mm.

The identified results demonstrate the proposed model-based 2D MUSIC damage identification algorithm possess the widely applicability of damage detection for composite plate with high precision and stability.

Table 1
The damage identification results of laminated composite plate.

Case	Actual positions		Identified positions		Error/mm
	x^*/mm	y^*/mm	x/mm	y/mm	
1	28	170	27	169	1.4
2	−100	100	−97	103	4.2
3	−50	100	−50	103	3.0
4	30	50	31	46	4.1
5	100	100	104	97	5.0
6	−50	150	−50	146	4.0
7	50	130	53	137	7.6
8	−50	50	−51	42	8.1

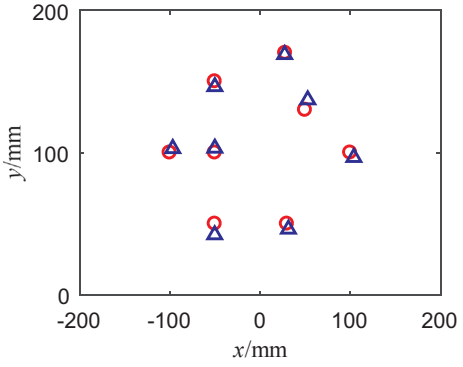

Fig. 8. The identified results of laminated composite plate (the red circle denotes actual damage position and the blue triangle denotes identified damage position). (For interpretation of the references to colour in this figure legend, the reader is referred to the web version of this article.)

5. Conclusions

The damage identification algorithm using guided waves based on improved MUSIC has been proposed for metal and composite plate-like structures. The propagation model of guided waves is considered to construct the spatial spectrum estimation MUSIC algorithm which is named model-based 2D MUSIC damage identification algorithm in paper. The proposed method combines the wave propagation model with MUSIC method under near-filed assumption. The proposed method can identify damages accurately as well as high resolution which is better than conventional MUSIC and DAS methods. In experimental verification, the damages have been successfully recognized with maximum location error 8.1 mm for laminated composite plate.

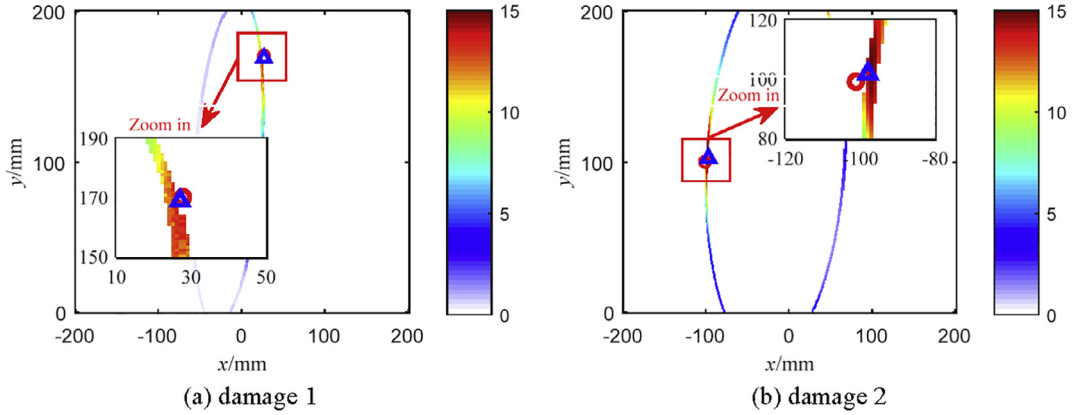

Fig. 7. The spatial spectrum of damage identified results for laminated composite plate (the red circle denotes actual damage position and the blue triangle denotes identified damage position). (For interpretation of the references to colour in this figure legend, the reader is referred to the web version of this article.)

Acknowledgements

This work is supported by the National Natural Science Foundation of China (Grant Nos. 51605365 & 51405369), the National Natural Science Foundation of Shaanxi Province (No. 2016JQ5049), the Key Research and development program of Shaanxi province (Grant Nos. 2017ZDCXL-GY-02-01 and 2017ZDCXL-GY-02-02) and the Young Talent fund of University Association for Science and Technology in Shaanxi of China (No. 20170502).

References

[1] Islam AS, Craig KC. Damage detection in composite structures using piezoelectric materials (and neural net). Smart Mater Struct 1994;3:1–9.
[2] Ferreira A, Roque C, Jorge R. Free vibration analysis of symmetric laminated composite plates by FSDT and radial basis functions. Comput Method Appl Mater 2005;194:4265–78.
[3] Zuo H, Yang Z, Chen X, Xie Y, Miao H. Analysis of laminated composite plates using wavelet finite element method and higher-order plate theory. Compos Struct 2015;131:248–58.
[4] Xu K, Ta D, Moilanen P, Wang W. Mode separation of Lamb waves based on dispersion compensation method. J Acoust Soc Am 2012;131:2714.
[5] Yang Z, Chen X, Li X, Jiang Y, Miao H, He Z. Wave motion analysis in arch structures via wavelet finite element method. J Sound Vib 2014;333:446–69.
[6] Su Z, Ye L. Identification of damage using Lamb waves: from fundamentals to applications. New York: Springer; 2009.
[7] Xu K, Ta D, Su Z, Wang W. Transmission analysis of ultrasonic Lamb mode conversion in a plate with partial-thickness notch. Ultrasonics 2014;54:395.
[8] Xu C-B, Yang Z-B, Chen X-F, Tian S-H, Xie Y. A guided wave dispersion compensation method based on compressed sensing. Mech Syst Signal Process 2018;103:89–104.
[9] Su Z, Ye L, Lu Y. Guided Lamb waves for identification of damage in composite structures: a review. J Sound Vib 2006;295:753–80.
[10] Jansen D, Hutchins D. Lamb wave tomography, Ultrasonics Symposium. Honolulu, USA: IEEE; 1990. p. 1017–20.
[11] Zhao X, Royer RL, Owens SE, Rose JL. Ultrasonic Lamb wave tomography in structural health monitoring. Smart Mater Struct 2011;20:1–10.
[12] Hay T, Royer R, Gao H, Zhao X, Rose J. A comparison of embedded sensor Lamb wave ultrasonic tomography approaches for material loss detection. Smart Mater Struct 2006;15:946–51.
[13] Wang CH, Rose JT, Chang F-K. A synthetic time-reversal imaging method for structural health monitoring. Smart Mater Struct 2004;13:415–23.
[14] Hall JS, Fromme P, Michaels JE. Guided wave damage characterization via minimum variance imaging with a distributed array of ultrasonic sensors. J Nondestruct Eval 2014;33:299–308.
[15] Hall JS, Michaels JE. Minimum variance ultrasonic imaging applied to an in situ sparse guided wave array. IEEE Trans Ultrason Ferroelectr Freq Control 2010;57:2311–24.
[16] Hall JS, Mckeon P, Satyanarayan L, Michaels JE, Declercq NF, Berthelot YH. Minimum variance guided wave imaging in a quasi-isotropic composite plate. Smart Mater Struct 2011;20:1–8.
[17] Zhao X, Gao H, Zhang G, Ayhan B, Yan F, Kwan C, et al. Active health monitoring of an aircraft wing with embedded piezoelectric sensor/actuator network: I. Defect detection, localization and growth monitoring. Smart Mater Struct 2007;16:1208.
[18] Tabatabaeipour M, Hettler J, Delrue S, Van Den Abeele K. Reconstruction algorithm for probabilistic inspection of damage (RAPID) in composites. In: 11th European conference on non-destructive testing (ECNDT 2014); 2014.
[19] Odendaal J, Barnard E, Pistorius C. Two-dimensional superresolution radar imaging using the MUSIC algorithm. IEEE Trans Antenn Propag 1994;42:1386–91.
[20] Lehman SK, Devaney AJ. Transmission mode time-reversal super-resolution imaging. J Acoust Soc Am 2003;113:2742–53.
[21] Vergallo P, Lay-Ekuakille A. Brain source localization: a new method based on MUltiple SIgnal Classification algorithm and spatial sparsity of the field signal for electroencephalogram measurements. Rev Sci Instrum 2013;84:1–7.
[22] Xu Y, Xue W, Li Y, Guo L, Shang W. Multiple signal classification algorithm based electric dipole source localization method in an underwater environment. Symmetry 2017;9:1–15.
[23] Schmidt RO. A signal subspace approach to multiple emitter location spectral estimation. California: Stanford University; 1981.
[24] Devaney AJ, Marengo EA, Gruber FK. Time-reversal-based imaging and inverse scattering of multiply scattering point targets. J Acoust Soc Am 2005;118:3129–38.
[25] Labyed Y, Huang L. Ultrasound time-reversal MUSIC imaging with diffraction and attenuation compensation. IEEE Trans Ultrason Ferroelectr Freq Control 2012;59:2186–200.
[26] Qian C, Huang L, So HC. Improved unitary root-MUSIC for DOA estimation based on pseudo-noise resampling. IEEE Signal Process Lett 2013;21:140–4.
[27] Liang J, Liu D. Passive localization of mixed near-field and far-field sources using two-stage MUSIC algorithm. IEEE Trans Signal Process 2010;58:108–20.
[28] Wang B, Zhao Y, Liu J. Mixed-order MUSIC algorithm for localization of far-field and near-field sources. IEEE Signal Process Lett 2013;20:311–4.
[29] Yang HJ, Lee YJ, Sang KL. Impact source localization in plate utilizing multiple signal classification. Proc Inst Mech Eng Part C J Mech Eng Sci 2013;227:703–13.
[30] Zhong Y, Yuan S, Qiu L. Multi-impact source localisation on aircraft composite structure using uniform linear PZT sensors array. Struct Infrastruct Eng 2015;11:310–20.
[31] Yuan S, Zhong Y, Qiu L, Wang Z. Two-dimensional near-field multiple signal classification algorithm-based impact localization. J Intell Mater Syst Struct 2015;26:703–4.
[32] Zhong Y, Yuan S, Qiu L. Multiple damage detection on aircraft composite structures using near-field MUSIC algorithm. Sens Actuators, A 2014;214:234–44.
[33] Zhong Y, Xiang J, Gao H, Zhou Y. Impact energy level assessment of composite structures using MUSIC-ANN approach. Struct Control Health Monit 2016;23:825–37.
[34] Engholm M, Stepinski T. Direction of arrival estimation of Lamb waves using circular arrays. Struct Health Monit 2011;9:467–80.
[35] Giurgiutiu V. Structural health monitoring with piezoelectric wafer active sensors (second edition). Brit J Ophthalmol 2014;58:438–54.
[36] Zhong Y, Xiang J. A two-dimensional plum-blossom sensor array-based multiple signal classification method for impact localization in composite structures. John Wiley & Sons Inc.; 2016.
[37] Levine RM, Michaels JE. Model-based imaging of damage with Lamb waves via sparse reconstruction. J Acoust Soc Am 2013;133:1525–34.
[38] Levine RM. Ultrasonic guided wave imaging via sparse reconstruction. Atlanta: Georgia Institute of Technology; 2014. p. 154.
[39] Zuo H, Yang Z, Sun Y, Xu C, Chen X. Wave propagation of laminated composite plates via GPU-based wavelet finite element method. Sci China Technol Sci 2017:1–12.